USE OF VERTICAL SODARS IN METEOROLOGY (REVIEW)

M.A. Lokoshchenko

M.V. Lomonosov State University, Moscow
Received November 10, 1995

Meteorological aspects of Doppler-free acoustic sounding of the atmosphere are considered. Numerous intercomparisons of acoustic radars (sodars) records with direct measurements with meteorological sensors in ABL are analyzed in detail. Summary is given of the results of sodar sensing use for air pollution monitoring, studying regional atmospheric fluxes, as well as mesoscale peculiarities in the horizontal thermal structure of the boundary layer (connected with heat islands over cities and others factors). Possibilities are discussed of using sodar records for the mixing layer height estimation, atmospheric fronts detection, etc. Much attention is paid to the works of Russian scientists.

1. INTRODUCTION

Acoustic remote sounding shows considerable promise in application to studies of the atmospheric boundary layer. It is based on the physical phenomenon of sonic waves scattering by turbulent atmosphere that was discovered by Tindall in 1873. Modern theoretical concepts on this phenomenon are summarized in Refs. 25, 30, and 44. In accordance with them, sound is backscattered by inhomogeneities of scalar fields, mainly by those of heat and moisture. If the wave number of such periodical inhomogeneities is within the inertial interval of the turbulent spectrum, then the cross section of sound scattering at 180° can be approximately expressed in terms of the temperature fluctuation structure characteristic C_T^2. The latter is the mean square difference of instantaneous values of temperature T at two points spaced at a unit distance.

The simplest pulsed acoustic radar (sodar) with a very low sounding range (100 m) was constructed in 1946 (Ref. 54). But in fact this method goes back to 1967. This is the time when McAllister discovered the sodar of modern type — with a matched transceiving antenna and continuous recording of return signal intensity in the time—height coordinate system with the Alden facsimile apparatus.[73] This was McAllister too, who succeeded in significantly decreasing the operation frequency, that allowed the sounding range to be widened up to 1.7 km.

At the frequencies about 1.5—1 kHz commonly used, this range is up to 1—1.5 km, as was predicted by Little.[47] Further decrease of the operation frequency results in a sharp growth of sound noise.[16] The range can be increased at the expense of sharp increase in the power of sounding pulse (Ref. 43 reports about 3 km range with total power of 2.7 kW). But McAllister's hopes to widen the capabilities of the acoustic sounding up to the tropopause level[74] are still not realized, and the ABL remains the natural region of this method application.

Monostatic sodars with one vertical antenna are used for observations under conditions of very polluted air over big cities and industrial zones. Doppler sodars (usually three-component with one vertical, and two tilted antennas) give an information about altitude profiles of wind field characteristics in addition to facsimile records of the thermal structure. They help to detect vertical wind shears dangerous for aviation.[44,64,81] Sodar data on the turbulence in ABL are also used in astrophysical investigations.[7] Long-term sodar observations are also helpful when planing construction in poorly studied regions.[68]

Information about thermal stratification of the lower atmosphere is of interest for meteorologists. In this review, possibilities and main directions of its study from the facsimile records of usual vertical sodars are briefly summarized. Study, with the help of these sodars, of turbulence characteristics, as well as consideration of other modifications of acoustic sounding (monostatic, Doppler, bistatic, and others) is beyond the scope of this paper.

2. DETERMINATION OF THE ABL STRATIFICATION FROM SODAR FACSIMILE RECORDS

The power of return signal, recorded by a vertical sodar is

$$P = P_0\, \sigma(180°) \left(\frac{c\tau}{2}\right) SR^{-2}\, L, \qquad (1)$$

where P_0 is the power of sounding pulse; $\sigma(180°)$ is the backscattering cross section; c is the speed of sound; τ is the pulse duration; $\frac{c\tau}{2}$ is the length of a pulsed scattering volume; S is the antenna area; R is the distance to scattering volume; L is the instrumental

0235-6880/96/07 616-13 $02.00

constant allowing for construction features of a given sodar (Ref. 16 and others). The response to the emitted pulse is shown in a facsimile record as a vertical bar. Each successive result is depicted immediately adjacent to the previous one and the degree of line blackening is proportional to the power of signal received from the corresponding height.

With the unstable ABL stratification ($\gamma = -\partial T/\partial z > \gamma_a$, where $\gamma_a = 0.98°C/100$ m) vertical images are typical for a signal in a facsimile record, namely, "feathers",[74] "columns"[52,74] "grass",[60,80] "roots",[61] "stalagmites",[82] etc., what is connected with the circulation in mesoscale convective meshes. These narrow bands of intense return signal correspond to regions of turbulent vortexes with large values of C_T^2. Usually[44,66,74] they are identified with the upward branches of meshes, while the gaps separating them in a facsimile record correspond to zones of downward flows, where cooler air portions fall down. At the same time, Parry et al.[77] came up with an idea that C_T^2 grows on the boundaries of upward flow, rather than inside it, where wind shear is observed as well as larger horizontal differences in the temperature field. However, comparisons with Doppler measurements of the vertical component ω of wind velocity have shown a good agreement of "feathers" images with zones of upward flows.[44,66]

The longest period of convective alternation on a sodar record (echogram) is usually equal to 10–15 min (Ref. 10). The turbulence structure in a separate feather is inhomogeneous and is characterized by C_T^2 growth from edge to center of this zone (i.e. there are feathers inside feathers).[59] The scanning time, when recording convective structures, usually correlates with the mean wind speed v in the ABL.[44,90] Reference 38 describes the convection observations with two high-frequency sodars, one of which was installed horizontally on a high mast.

Near-ground and elevated inversions usually manifested themselves on echogram as clear, turbulized images — horizontal layer of blackening. In accordance with the gradient Richardson number

$$\mathrm{Ri} = \frac{g}{\Theta}\,\frac{\partial\Theta/\partial z}{(\partial v/\partial z)^2} \qquad (2)$$

(Θ is the potential temperature), the dynamic turbulence can be developed due to vertical wind shear in slightly stable ABL and even under inversion conditions ($\gamma < 0$), if $\mathrm{Ri} < 0.25$. In the region of this shear, separate air portions with different Θ will be mixed; as a result, fluctuations of T will be of the same order as fluctuations of v. Just these "stimulated" inhomogeneities in the field of T create a return sound signal in a stable ABL.[44,90]

The return signal power, showing itself as a degree of blackening on a sodar record, is proportional to a backscattering cross section σ(180°), Eq. (1), which in its turn depends on the structure characteristic of the acoustic refractive index; the structure characteristic is usually close to C_T^2 in value. As to the latter, taking into account the refraction effects, it is related to the potential temperature gradient in the stable ABL:

$$C_T^2 = a^2\, L_0^{4/3}\, (d\Theta/dz)^2. \qquad (3)$$

Here L_0 is the outer scale of turbulence, inversely proportional do dv/dz. Tatarskii derived Eq. (3) for the case of passive conservative impurity mixing. Inhomogeneities of T in the shear field can be considered as this impurity as well. It is clear that estimates of inversion intensity from the degree of record blackening (following the advice given in Refs. 8 and 77) can be only approximate, because at different $\frac{dv}{dt}$ values and the same vertical temperature lapse rate γ, the power P proves to be different. In Ref. 15 the uncertainty in the influence of the wind shear and mixing, it creates, on the return signal was noticed in Ref. 15.

This is the commonly accepted explanation for the nature of sound waves scattered in the air layer where $-\partial\Theta/\partial z < 0$ or even $\gamma < 0$ (inversion). However, direct measurements of T and v profiles within inversions, especially near-ground ones, give sometimes very large values of Ri (see Ref. 66).

But even in these cases, as will be shown below, turbulized images of the inversion regions are seen on sodar records. The reasons for this are not yet completely known. It is believed that in separate local zones inside the inversion the value of Ri remains less than 1/4 (Ref. 44). The possibility that turbulence keeps under superlarge values of Ri is problematic. Destruction of internal waves in ABL or other processes can be additional sources of turbulence.[4]

At neutral stratification or a very slight wind shear in stable ABL, there are no images on sodar records. In the first case $\gamma = 0.98°C/100$ m and $\partial\Theta/\partial z = 0$. Under these conditions $C_T^2 = 0$ (Eq. (3)) and according to Eq. (1) no return signal is formed. That is why sodar is incapable of recording thermal turbulence in a neutral ABL.

Identification of ABL stratification from the viewpoint of turbulent structures on a sodar record is an indirect method. It is necessarily subjective due to visual interpretation of records, widely accepted up to date in spite of numerous attempts to automate the facsimile information processing.[5,69] But uncertainty of that qualitative analysis is small on the whole, because questionable and uncertain, in morphology, images are mainly assigned to transient periods of a day. Thus, evening formation of near-ground inversions can be usually followed with a sodar accurate to 0.5 hour (Refs. 20 and 61), i.e. with the error about 5% of their total repetition. Morning elevation of the inversion layer from the ground is manifested as a distinct light gap in a lower part of a record at a time lag of 1 (Ref. 74) or 1.5 hour (Ref. 60).

3. COMPARISON OF SODAR DATA WITH DIRECT MEASUREMENTS IN ABL

Vast experience has been accumulated on comparing sodar facsimile records with data of direct measurements of meteorological elements in the ABL. Usually either general qualitative view of a turbulent structure on a record and the value of γ in this layer or characteristic heights of sodar images and the singularities at T and v vertical profiles are compared. Let us generalize the results of these comparisons separately.

Ideal one-to-one relations between sodar images and ranges of γ values cannot be established, since the value C_T^2 depends not only on γ. Besides, humidity fluctuations sometimes play a marked role in return signal formation too.[83] Table I summarizes the attempts to establish, although approximately, such relations.

TABLE I. Correlation between the view of sodar facsimile images and the vertical temperature lapse rate $\gamma = -\partial T / \partial z$ *in the lower air layer* (°C /100 m).

Sodar record	Ref. 34	Ref. 8	Ref. 88
vertical feathers	$\gamma > 1.0$	$\gamma \geq 1.2$	$\gamma > 1.0$
lack of a signal	$0.0 < \gamma \leq 1.0$	$0.5 \leq \gamma < 1.2$	$0.2 \leq \gamma \leq 1.0$
weak nonordered		$-0.3 \leq \gamma < 0.5$	–
horizontal layers	$\gamma \leq 0.0$	$\gamma < -0.3$	$\gamma < 0.2$

In Refs. 34 and 60 the type of sodar images is compared to the data of radiosondes and balloonborne measurements in Japan (see the table). In one of the three measurement sites, weak images prevailed in a wider range of γ: from – 0.2 to 1.2, although in the range from 1.0 to 1.2 there were mainly blurred feathers. Sometimes well pronounced feathers showed themselves beginning already from $\gamma = 0.4$, and sometimes there were no signals even in the layer of intense inversion up to $\gamma = -6.4$°C/100 m (seemingly, at a very slight wind shear). Well stratified structures sometimes manifest themselves not only from inversion but in a weakly stable ABL as well.

Zhukov et al.[8] related the view of sodar images to the value of γ in the lower 100-m layer based on the data of *in situ* measurements from the TV tower in Moscow. They also related the tone of horizontal layers to γ (light gray layers were observed on records at $-0.3 \leq \gamma < 0.2$; dark gray layers were observed at $-1.2 \leq \gamma < -0.3$; and black layers were observed at $\gamma < -1.2$). However the reliability of γ determination based only on the tone of facsimile images is rather questionable.

In Poland[88] 74 balloonborne measurements of γ were compared with the view of sodar records. It is omitted however whether the correspondence worsens at any small change of boundaries of γ ranges. It is not also clear to what type the transient images between the absence of a signal and clearly seen layers are assigned.

On the whole, the results of comparison show good agreement between the view of a sodar image and the type of temperature stratification. In the unstable ABL, well distinct vertical feathers are seen on a record; in neutral or weakly stable ABL there is no signal, whereas in a more stable boundary layer weak images of transient type can be noticed. Inversions are usually related to the presence of horizontal layers of clearly seen blackening on an echogram.

In Refs. 82 and 83 the detailed classification of sodar images was developed by their correspondence to the Paskvill classes of stability determined by the wind direction fluctuations. These classes certainly have no one-to-one correspondence with the value of γ. About 1000 hours of sodar records in India were analyzed. The majority of classes proved to be related simultaneously to several views of images, which differed in many details: layers with smooth or rough, in time, top; high or low feathers, etc. However, as in Ref. 8, Ref. 88 gives no statistical data on the closeness of relations obtained.

Let us now consider comparisons of facsimile images of inversion layers with the vertical profiles of meteorological parameters. Such a correlation was made for the first time in 1968, when the sodar was installed 500 m apart a radio tower.[74] The facsimile records with thermo- and anemograms at 75 m level superimposed on them are presented. The profiles of T from the results of mobile carriage runs from tower bottom to top are presented separately. The correspondence of horizontal layers of blackening to inversion is shown, as well as that of vertical feathers to unstable profile of T near the ground. At night the layer of blackening was clearly seen on a record when the wind speed reached a threshold value at an altitude of 75 m. Although the authors did not study specially the altitude correlation, at least good qualitative correspondence of morning elevation of the inversion layer to the shape of temperature profiles is demonstrated.

Reference 43 presents, for the first time, the echogram, on which the profiles of T and relative humidity f obtained from the radiosonde data are superimposed. Inflections on these profiles coincide

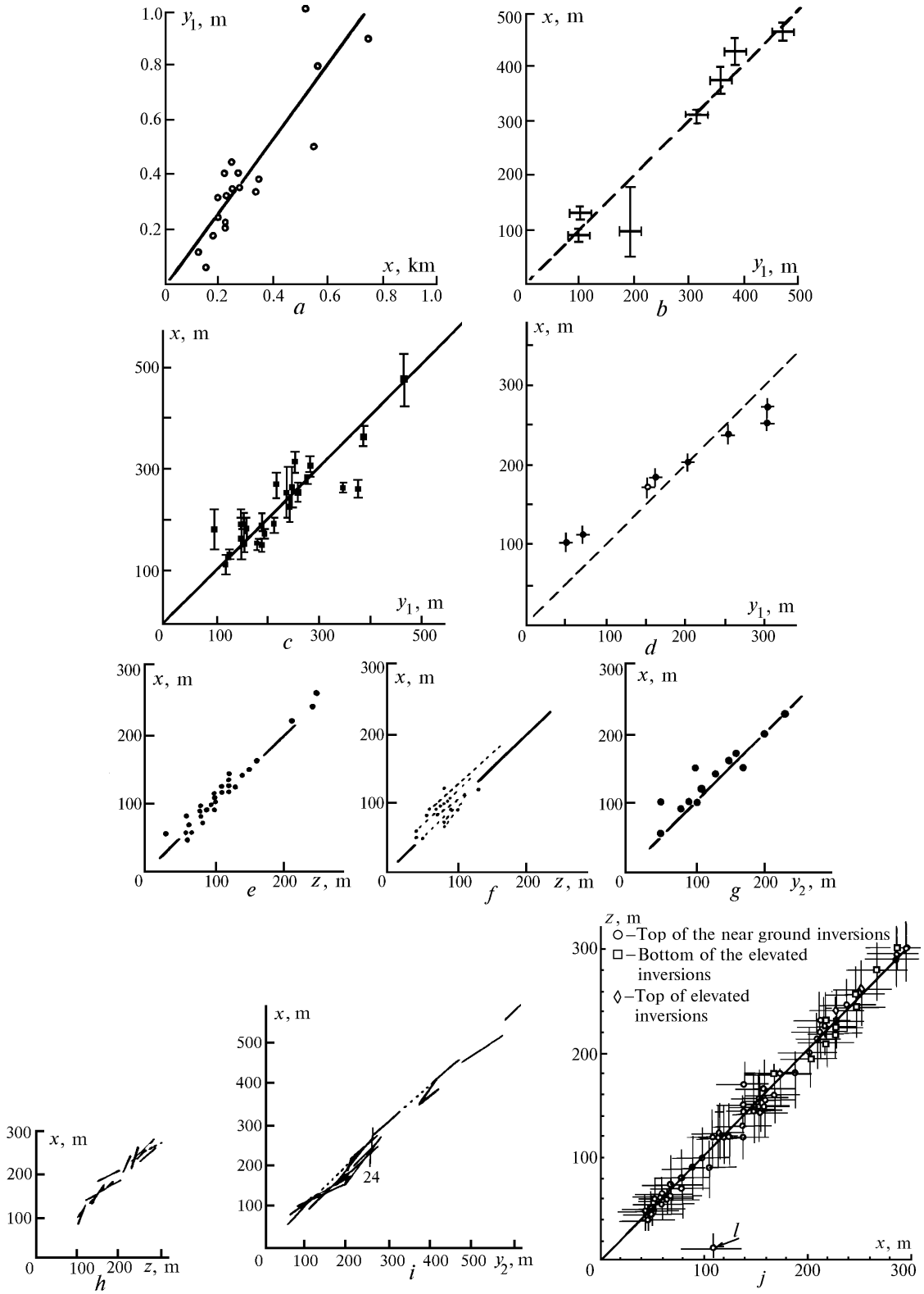

FIG. 1. Experimental correlation between gradient and sodar estimates of the boundaries of inversions in the ABL; x axis is for sodar data, y_1 is for standard radiosonde data, y_2 is for low-level radiosondes, and z is for tethered aerostat; data of Wyckoff et al.[91] (a), Goroch[56] (b), Hicks et al.[61] (c), Guedalia et al.[58] (d), Hayashi and Ikeda,[34,60] measurements in Cukuba (e), Hayashi and Ikeda, measurements in Kashim (f), Hayashi and Ikeda, measurements in Kushiro (g), Hayashi and Ikeda, measurements in Cukuba (h), Hayashi and Ikeda, measurements in Kushiro (i) (Figs. 1e, f, and g are for near-ground inversions, and Figs. 1h and i are for elevated inversions), von Gogh and Zib[55] (j).

well with the sodar images of settling inversion in cyclone periphery. Above this layer f sharply drops by 40–50%.

Such correlations for near-ground inversions were summarized for the first time in the USA[91] on the basis of data from 19 radiosondes. Sodar estimates of the inversion power turned out to be underestimated on the average by 1/4 (Fig. 1*a*). It should be noted that with due regard for a large spread of values the sample was small in size. As the authors of Ref. 91 believe, the causes of such a trend are both change of sonic speed with height and errors due to sensors time lag while sonde goes up. But the first factor can contribute into the total error no more than 3%. At the same time, the authors omitted the fact that sodar image of a layer not always is identical to the inversion region, although the example of sodar record presented in this paper illustrates this clearly. The black layer on this record coincides with the zone of sharp growth of both v and T with height. Above this layer the weak inversion exists, but there is already no wind shear and so there is no return signal.

Reference 56 describes the comparison of T profiles obtained with usual USA military radiosondes and the heights of elevated inversions in the morning obtained from sodar data (Fig. 1*b*). In six of seven cases the agreement looks close, but the sample size is very small.

Reference 61 compares the sodar estimates of near-ground inversion boundaries with the data of 26 standard sondes launched 400 m from the site of sodar installation in Calgary (Fig. 1*c*). Vertical bars show the variability of inversion power as sodar gives for the 5-minute period of sonde being flown. Quite close correlation of estimates is seen as well as their good correspondence to the straight line. It can be seen, however, that when the upper point is excluded, a small discrepancy appears as well as in Ref. 91. At the same time, similar comparison for elevated inversions revealed no agreement between estimates. The same result was obtained in Ref. 3 too. One should keep in mind, in this case, low resolution of usual radiosondes and their low accuracy when measuring inversion boundaries at some heights, especially, for very thin layers.

One more comparison, in Canada,[51] involves the data of 33 sondes launched at the moment when sodar detected near-ground inversions. In this case estimates are very close to each other; underestimation of inversion power given by sodar is about 15% in winter and practically vanishes in summer (there is no picture here). In Ref. 58 all near-ground inversions detected by radiosondes were noticed on sodar echogram too. Sodar estimates of their power are somewhat underestimated for altitudes from 200 to 300 m (Fig. 1*d*).

Contradictory of the first results of comparison can be partially explained by low resolution of usual radiosondes; momentary readings against them being in free fly; sensors time lag in so doing; complexity of fine reference, to sodar record, of the moment when sonde comes through the top of inversion; as well as often the small size of samples. By the end of 1970s however more careful comparisons of sodar images with already more accurate results of measurements in ABL become known.

In Refs. 34 and 60 the sodar sounding was made simultaneously with the measurements in two sites with tethered aerostat and the low-level radiosondes in the third site. The advantages of aerostat measurements are their higher vertical resolution (10–50 m) and the possibility to make several readings at every level. Moreover, sound re-reflection from an envelope draws, on the sodar record, the trajectory of aerostat going up as a characteristic track, that makes the time reference more easy.[34,88] For more accurate reference, Hayashi and Ikeda averaged the heights of inversion boundaries by sodar for 10 minutes before and after aerostat started. Comparison of estimates for both near-ground (Figs. 1*e*, *f*, and *g*) and elevated inversions (Figs. 1*h* and *i*; separate layers are given as segments) shows everywhere their very good correspondence to one-to-one line. Sample size in this case is from 13 to 29 simultaneous measurements. The example is also given (Fig. 2) for the record of lifting of radiative inversion in the morning with T isopleths superimposed onto it. The isopleths were obtained from measurements at a high mast. The boundary of black layer on the record corresponds to the level of a sharp slowing down of the temperature growth with height, although very weak inversion, close to isothermy, extends higher, up to about 50 m.

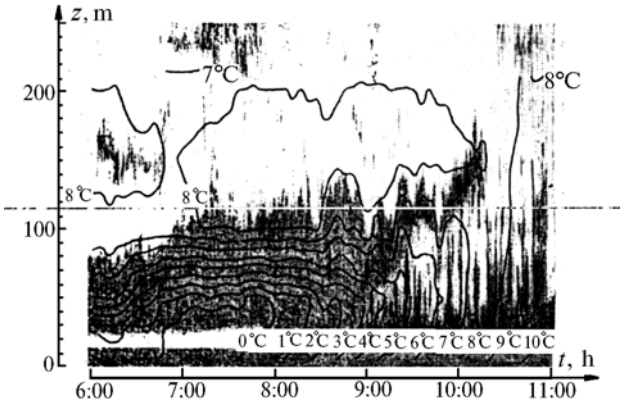

FIG. 2. Morning elevation and break out of the radiative near-ground inversion.[34,60] *Temperature isopleth from measurements at a high mast are superimposed on the sodar facsimile record. The axis t is for time, and the axis z is for height.*

Reference 55 presents data of the comparisons between aerostat measurements of T and v in SAR with the boundaries of inversion layers estimated from sodar data in the range 40–350 m. The resolution is 15–30 m for aerostat data and 30 m for sodar ones. The layer boundaries are referred to the points of inflection on T

profiles, where $\partial T/\partial z$ changes its sign and the sum of absolute values of differences between T readings at adjacent levels is below 0.4°C. Figure 1*j* shows 45 measurements of tops of near-ground inversions, as well as 12 and 2 measurements of bottoms and tops of elevated inversions. One can see an excellent agreement between estimates with a very close correlation without discrepancies. In only one case, the boundary of the black layer in the sodar record (110 m) is more closely related to the change of $\partial v/\partial z$ rather than $\partial T/\partial z$. In this case the isothermy was observed from 30 to 200 m, and the greatest wind shear was noticed between 90 and 120 m. In one example, more the images of near-ground and elevated inversions are separated by a clearly seen gap on the record, although T in this interval dropped by only several tenths of degree. Thus the results of Ref. 55 are evidence in favor of correlation between heights of sodar images and inflections of temperature profiles.

In Ref. 69, the presence of inversions (apparently elevated ones) was detected by maxima in vertical profiles of return signal intensity. Agreement between heights of such maxima from sodar record with the inversion boundaries from aerostat data proved to be very good. But it is not clear from this reference which heights of inversions were compared.

As one can see, the comparisons of sodar data with more accurate direct measurements of T have demonstrated much more close agreement than in the case with the data of usual sondes at early stages of these studies. However it is still problematic whether the sodar images always can be explained in terms of the ABL thermal structure only. In other words, it is unknown for what seasons and geographical conditions this conclusion is true.

It seems to us that the coincidence of the layer boundaries in sodar records and real inversion is possible with only an intense wind shear over the whole its area. But the maximum of low-level jet stream can be inside an inversion as well. In Obninsk for example, it takes place in each tenth case.[32] In this case the sodar may cut off the inversion, i.e., underestimate its real value (Ref. 89 and others). Therefore, the discrepancy between results is connected, in addition to other factors, with the climatic features of the ABL in different places. The agreement between estimates are closest in such cases, when the near-ground inversions are not well developed in vertical direction and v grows monotonically within them. This is observed for maritime conditions in mid-latitudes,[34,55,60] as well as in the Canada internal regions during warm period.[51,61] As to the winter, in that season of continental climate the inversions have higher power and often a complicated multilayer structure. In some their zones the Richardson number, Ri, is very high with wind shear weakening. The sodar image of near-ground inversions in this case is split into separate layers, cut-off in height, or underestimated as a whole. Naturally, the conclusions on underestimation of sodar data on inversion power were drawn in winter in the internal continental region.[51,91] Their true error is not so high, because sondes themselves overestimate the inversion top due to the sensors time lag.

Sodar images of elevated inversions were also many times compared with inflections on T profiles. In Refs. 49 and 51 the black layer on sodar record corresponded to only the bottom and the lower part of elevated inversion which had higher power as it followed from the data of individual usual radiosondes. But later, in the case of near-ground inversions, the agreement between different methods was demonstrated to be very good for both separate examples[43,45,52,63,77,91] and series of observations.[55,56,58,60] Interesting and ingenious examples of close correspondence between such estimates are presented in Ref. 57. At the same time, in Ref. 58 some elevated inversions above 500 m height were not detected by sodar due to strong attenuation of sound. Reference 43 also presents an example of the inversion at the altitude up to 2 km that was not detected by usual sodar but was noticed with a higher-power acoustic radar. Some peculiarities in sodar images of elevated inversions of different origin are considered in Refs. 21, 44, and 47.

As to the height of vertical feathers on sodar records, it can certainly be underestimated as compared to the thickness of convective ABL and can serve as its only circumstantial characteristic (excluding cases when the instrumentation with very powerful pulses is used[77]). This is connected with the fact that scattering of sound at frequency about 1 kHz is limited by inhomogeneities of only inertial interval of turbulent spectrum. In Ref. 82 the feathers' height, x, was compared with the mixing layer height by Holtzvort, y, calculated on the basis of daytime radiosonde sensing. The empirical expression: $Y = 4.24X + 95$ (in meters) was derived. Certainly, this estimate is connected with the contrast of a specific sodar and climatic peculiarities of India. However, similar estimates for Moscow conditions[22] turned out to be very close to that.

4. CLASSIFICATION OF SODAR FACSIMILE RECORDS

Wide variety of turbulent images on sodar records requires their systematization for solution of certain problems. The number of different codes for such data is now great enough. The lack of standards in this area makes the comparison of results very hard. Apparently, the general principles used when developing such schemes may be the following:

1) clear and unambiguous separation of turbulent images by their morphology, that allows the subjectivity of the analysis to be reduced to minimum;

2) in meteorological studies, the justified relation between the classes separated and ABL stratification;

3) choice of the optimal number of taxonometric units sufficient for characterization of the main types of

atmospheric stability and, at the same time, without excessive complication of the scheme;

4) possible separation, along with the main classes, their versions, describing additional peculiarities of a structure (tone, degree of manifestation, character of image boundary, etc.).

Fukushima et al.[52] distinguished only three classes: layers, waves, and feathers. This scheme is based on the relation of images to dynamic characteristics, and it can hardly be interpreted from the viewpoint of ABL stratification. There is no clear-cut criterion for distinction between layers and waves at oscillations of horizontal image in time. It is also unclear to what of three types the morning convection closed under the inversion layer (which in this case often is perturbed by oscillations) should be related.

The classification by Clark et al.[47] includes 14 types (in fact, only 13). One of them — feathers — is related to convection; other 12 types correspond to combinations of near-ground and elevated layers. The types are distinguished by pairs depending on the power of near-ground layer, degree of the top roughness, gap between layers, their vertical trend. The authors themselves believe that the advantage of this scheme is its richness in details. Many types are related to specific meteorological processes, but one-to-one correspondence of such an interpretation is not always beyond questions. Some types are evidently excessive. At the same time, the cases of closed convection, affecting pollution dispersal, (in Fig. 2 — from 9:00 to 10:00 L.T.) are not considered separately.

The classification presented in Ref. 79 is much more simple, because it is oriented to the study of atmospheric pollution. On authors' opinion, it is impossible to reveal real effect of one or other complex profile and details of sodar images upon pollution. Therefore only five classes are distinguished, to the last of which all complicated cases are referred. If the scheme in Ref. 47 is overloaded with quantitative criteria, here they are deficient (for example, when defining a small gap between layers). On the whole, this scheme[79] is concise and takes into account the connection with the ABL stability. Its weak point is the record of elevated inversions because the cases with them fall within three last classes simultaneously.

Hayashi[60] started from three main types of images, and then he developed a more detailed scheme. For each class separately, he distinguishes images into intense and weak, marking their code by capital or smaller letter. In addition, he characterizes the trend of height change on records. Such a two-stage scheme, which allows one to take into account minor peculiarities of images separately from their main distinction, is undoubtedly a step forward. The relation of distinguished classes to atmospheric stability is evident. It is only unclear whether this scheme can take into account simultaneous existence of near-ground and elevated inversions separately.

Very simple scheme by Walczewski[88] includes only four types. Its advantages are conciseness and connection with stratification of the ABL. The limitation is again neglect of elevated layer under near-ground one as the isolated situation. Similar simple schemes were proposed by Hicks et al.,[61] Krasnenko and Fursov.[17,19] The classifications by Pekour et al.[11,27] and Maughan[71] are somewhat more detailed (nine and eight classes). Very detailed schemes were proposed by Singal et al.[83] and Thomson.[67] The main distinctive criterion in them is related to stability of the ABL. Allowance for additional peculiarities in morphology is like in Clark's classification (thus, Singal denoted separately layers with different degree of top roughness, Thomson did this for layers with different trends to tilt, etc.). Singal also distinguished the images of layers in the form of a set of points, connected with the influence of humidity characteristics on sound scattering.

5. APPLICATION OF SODARS TO MONITORING OF ATMOSPHERIC POLLUTION

Rapid attenuation of sound restricts the sounding range of medium-power sodars to boundaries of the ABL — the natural reservoir of atmospheric pollution. Therefore most often they are used for monitoring of the state of air medium. The literature on this subject is quite numerous. Examples and qualitative conclusions give way to statistical generalization of correlations between sodar data and pollution indices.

Wyckoff et al.[91] present the examples of echograms for the cases of "dangerous pollution". The authors give no concentrations and even do not explain what type of pollution they say about. Nevertheless, they noticed a lot of interesting features: sharp growth of pollution near ground when sedimentation inversion merges together with the near-ground one, clearing of the lower layer from pollutants two hours after destruction of the near-ground inversion, etc. Considered is the example of pollution during three days, which was connected with the continuous existence of inversion near ground and at low heights.

In the same years Beran and Hall[41] generalized a wide variety of possible sodar applications in an abstract city or industrial zone and analyzed its advantages over other methods.

Prater and Colls[79] have compared the concentrations of sulfur dioxide and solid particles near Cleveland (United Kingdom) with the power of near-ground inversions, detected in the same region with a sodar. All hourly measurements of power were divided into altitude intervals each 25 m thick, and for each of them average concentrations were calculated. In such a manner, 3000 hours with near-ground inversions were analyzed with simultaneous measurements of SO_2 (Fig. 3) and soot. Both cases demonstrate the concentration increase as inversion thickness increases up to 200-250 m; and for wider inversion the data spread is seen with the general trend to pollution dispersal. It is obvious that the wider is inversion, the more pollution sources are encompassed by its layer.

The largest effective heights of industrial stacks in this area are 170—200 m.

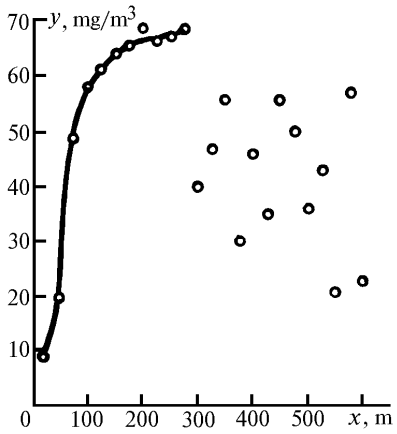

FIG. 3. Correlation between the hourly mean concentrations of SO_2 (y axis) near ground and the thickness of the near-ground inversion[79] *(x axis).*

Russel and Uthe[80] studied the conditions of ozone and soot accumulation near ground in the region of San Francisco bay. Sodar records are presented that were obtained simultaneously at three sites during one week, as well as T and v profiles in these days. These facsimile records were used to obtain: 1) the mixing layer height, i.e. the bottom of elevated inversion which usually restricts here the layer of marine air, 2) the mixing intensity (qualitatively — by the presence or absence of feathers on a record). The authors noticed good, on the whole, correlation between the pollutant concentrations and mixing layer characteristics by sodar. However this author's conclusion is not obvious. Under close examination of materials presented one can see that the pollution levels depend on the wind velocity more strongly than on temperature stratification. Thus, in the first two days sodars continuously recorded a low near-ground inversion, hampering the dispersal, but the concentration remained not high at a moderate wind. In the next two days the situation became better from the point of view of thermal structure, especially, by the fourth day, when in the afternoon at all sites the convection was observed, not closed by inversion at height. Nevertheless, the conditions close to calm resulted in a sharp increase of pollution near the ground.

Guedalia et al.[58] used acoustic sounding and radon measurements to estimate the coefficients of turbulent exchange in a stable ABL. The radon concentrations were measured at the center of town and 8 km apart. Sodar worked at both sites alternatively. Having estimated the real mixing layer height (i.e. the height of the elevated inversion bottom) in the morning from sodar record, the authors calculated the radon flow from the difference in its concentrations and then the equivalent mixing layer height, H_e, the characteristic, connected with the intensity of vertical diffusion in a stable ABL. The H_e values obtained were then compared with the height of night inversions, estimated from sodar data.

The ozone concentration decreases at night in the near-ground inversion layer due to chemical sinks of O_3 near ground and abruptly increases to its top. The possibility to estimate the upward ozone transport from the values of its near-ground concentration in the morning at the moment of inversion destruction was studied, in Ref. 40. Using four sodars displaced along the USA shore line from Washington to Boston, the mixing layer height and the time of inversion vanishing in the morning were followed.

Reference 42 demonstrates the connection, between the ozone concentration and changes in the ABL stratification from sodar data during a day, as well as the correspondence of abrupt changes in O_3 vertical profiles to the areas of inversions on sodar records.

Krasnenko et al. have conducted simultaneous observations with sodar and polarization aerosol lidar in Tomsk (USSR). The sodar record with the image of elevated inversion is presented in Ref. 16. The isopleths of the backscattering coefficient of atmospheric aerosol, superimposed on it, demonstrate the aerosol cloud under the bottom of turbulized layer. The correlation coefficient between the height of inversion bottom and this cloud top was 0.9. Once the sky became clear and air warmed up, the fine water aerosol comprising this cloud evaporated, but the inversion persisted. In the same manner, Ref. 18 demonstrates the aerosol accumulation already under near-ground inversion.

Reference 19 presents the results of sodar sounding with simultaneous measurements of CO_2, O_3, and NH_3 with a long path absorption gas analyzer. Based on these measurements in Tomsk during 7 hours of a day, the correlation coefficients were calculated between the mixing layer height (MLH) estimated from sodar data and the concentrations obtained. However, their reliability is under question because of a small sample size. In addition, the authors evidently identified MLH at convection in day time with the height of feathers on sodar record,[5] that resulted in underestimation of the MLH.

In Ref. 31 the view of sodar record in Moscow is compared to the CO measurements 2 km apart from sodar installation. These measurements were performed in the same way as in Ref. 19 and also establish the connection between the CO concentrations obtained and the passages of separate convective thermics on the sodar record.

Reference 6 compares the thickness of near-ground inversions in Moscow estimated from sodar data for one month with CO concentration. Although rather a wide spread of data is evident, the authors drew the conclusion about unambiguous decrease of CO concentration with inversion layer growing. This contradicts the result of Ref. 79 for SO_2, that can be explained by the decisive contribution of low sources into the total air pollution in Moscow. Reference 14 investigates the air pollution with soot aerosol in

Moscow. Its concentrations at the city center were, on the average, 10% higher than in the outskirts. Their connection with both v and temperature stratification estimated from sodar data was discovered. The soot content is lowest with no near-ground inversions occurred in winter and in the period of day-time convection in summer, especially at invasion of arctic air masses. The pollution increase at rain was noticed, as in Ref. 6.

The limited volume of this review does not allow me to mention all the papers on this subject, see for example, Ref. 84 and references therein. At present sodars are effectively used in routine monitoring of pollution. Thus, Ref. 89 describes the introduction of sodar equipment into the system of 12-hour forecast of SO_2 concentration fields in Upper Silezia. At unfavorable stratification of the ABL, coal with reduced sulfur content is used, and some technological processes are promptly discontinued. In SAR acoustic radars are used to follow the conditions of atmospheric stability, influencing the operation of dry cooling equipment of power stations.[87] In the industrial zone of Kemerovo (USSR) sodar was used for prompt warning in the cases of dangerous air pollution.[5]

6. SODAR STUDIES OF THE ABL HORIZONTAL STRUCTURE

Sodars are also used for studying local regularities of the ABL spatial structure, for example, influence of a big city, as well as peculiarities of local circulation, manifesting themselves as wind shears and inversions at low heights. To this end, simultaneous operation of several sodars at different sites or fast transportation of one sodar along a given profile with short stays for sounding in each point is organized.

The vicinity of Christchurch (New Zealand) is ashore the Pacific Ocean near the Southern Alps slopes. The boundary of shear of the warm foehn wind from these slopes and the cold oceanic breeze forms an elevated inversion, seen on sodar records. To the south of the town the low Port hills are situated. Under conditions of south-west wind from the Southern Alps and progressive lowering of the shear boundary, the movable setup with sodar has moved around the path 35 km long joining eight sites four times for 10 hours (Ref. 86). At each point the sodar operated during 10 minutes. In the neighboring reference point the sounding was made with the second sodar. Using the linear interpolation of the data, the maps of the elevated inversion surface over the town were constructed for every hour (Fig. 4). On the whole, this surface lowered progressively, keeping the general slope to the ground in the direction to the center of the island, i.e. to the Southern Alps. However, having reached the height of the Port hills the surface exhibits an abrupt and closed reduction over town, that is likely the result of the katabatic winds from their tops. The profile of the near-ground inversion thickness constructed also revealed its increase in the eastern direction to the ocean.

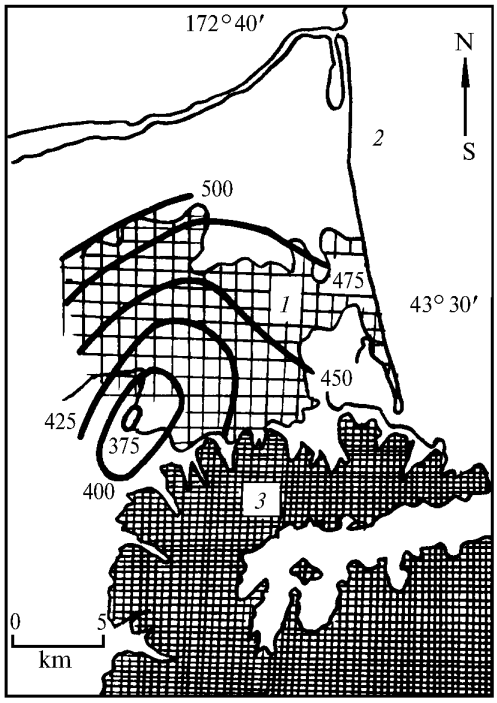

FIG. 4. Map of the wind shear boundary surface connected with the near-ground inversion in the region of Christchurch (New Zealand) at 12:00 of March 5, 1979, estimated from the sodar data[86] (in meters): Christchurch (1), Pacific Ocean (2), Port hills (3).

Some time later Surridge repeated the experiments with a movable sodar in the region of Johannesburg in SAR.[87] He obtained the profile of the night near-ground inversion thickness under conditions of general slope of the surface to the sea level. It turned out that the absolute height of the inversion top is not constant at different points too and it generally follows the terrain profile. However, it is so only partially, since over local dips its thickness was somewhat greater than over elevations. The greatest thickness was observed at two points in the center of the city.

Simultaneous observations with two sodars in the Alberta Oil Sands (Canada) were followed with aerostats and radiosondes.[51] Both sodars operated 4 km apart from each other. Differences in conditions at two points (closeness of one of them to the river) manifested themselves, among other things, in the greater number and higher degree of blackening of turbulized elevated layers on the facsimile record for that point. The observations with four sodars at the north-east of the USA[40] showed that morning inversion was broken up in Washington on the average by a half hour later than in Boston. Based on sodar data and radon measurements at two points,[58] the indirect conclusion was drawn on thicker night near-ground inversions in suburb as compared to a city center.

In Ref. 39, based on the data of long-term, albeit in different years, sodar observations, the peculiarities

of ABL stratification were considered at three different points: at a mountain top, in a valley, and in the center of a big city (Athens).

Synchronous observations with two and three sodars were also performed in the Moscow region.[9,12,23,28,78] The influence of a big city as a mesoclimatic object upon the ABL structure has been demonstrated. The repetition of near-ground inversions decreases regularly, whereas that of convective stratification increases when going from periphery to center. In the center, the inversion layer breaks away from the ground in the morning 1 hour earlier and forms in the evening 2 hours later than outside the city. In the city center, near-ground inversions are thicker (as the data from Ref. 87 show) due to a more intense turbulent exchange.

Synchronous sodar observations were also performed for two years at the center of London and outside it.[85] The city influence also manifested itself in a more frequent convection and a more rare neutral stratification. But it is hard to believe that there are no near-ground inversions in London at all, even with regard for influence of the city island of heat.

7. ATMOSPHERIC FRONTS DETECTION

It is hard to unambiguously separate the inversions connected with fronts. The frontal surface itself, dividing air masses, not always can be seen on echogram.[21] In anafront at upward sliding of warm air such inversions often vanishes. In other cases, the layer image on a record is masked by the turbulence strengthening in the front zone and acoustic noise at precipitation.

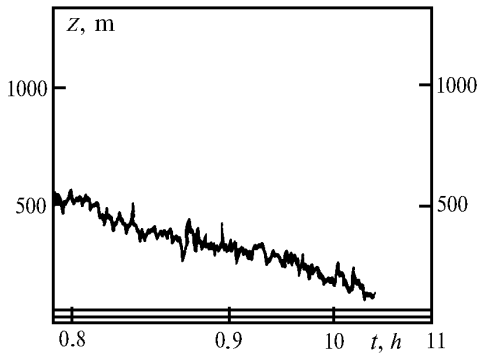

FIG. 5. An image of the warm atmospheric front passage on the sodar record.[61] *The t axis is for time, and z axis is for height.*

However frontal inversions are often mentioned in the literature devoted to sodars. These are, for example, downward tilted layer as the record goes on, at the warm front passage[61] (Fig. 5) or upward layer in the case of cold front passage.[50] Reference 53 summarizes 26 such images recorded in India and France. But to provide a support for such an interpretation of these layers as front surfaces, these papers give neither barogram recorded simultaneously nor some synoptic information. Similar situation holds in Ref. 76, which presents the satellite picture made 18 hours after the observation of inversion at the South Pole and 500 km apart from the point of observation. This picture, displaying the cyclonic vortex, cannot be considered as a strong evidence of a frontal character of the inversion observed. Most likely, just the lack of rigorous criteria in definition of the front is the reason for recording sometimes downgoing layers at a cold front passage, as well as the front tilt angles, calculated from sodar record, which amounted to units and even tens of degrees.[53] At the same time, an interesting example of frontal inversion at height in the zone of wave action at the Polar front is presented in Ref. 77. The connection between the layer recorded by sodar and the air masses interface is confirmed by the fragment of the synoptic map. However, other explanation of a similar example in the same paper seems to be ambiguous. It is obvious that the possible sodar images of front surfaces is of great interest. But every such case needs for a close inspection.

8. STUDY OF SYNOPTIC PECULIARITIES IN THE ABL STRATIFICATION

High resolution of sodar data allows their use in detailed analysis of connections between the ABL structure and synoptic conditions. But this research direction has not been adequately discussed in literature. Some examples demonstrate only the influence of advective factors upon the repetition rate and height of convective images. This item has to be considered in a more detail. Thus, the sodar record with clearly seen feathers was obtained even at the South Pole.[44] The reason for convection development was the invasion of the cold air mass with $T = -40°C$ on the relatively warm ($T = -30°C$) ice surface. Quite different situation was observed near Tsimlyansk (Russia).[10] In one of the days of observation the feathers on the record turned out to be weakened in the evening 4 hours earlier than usually. That calming of convection was the result of invasion of warm air from steppe areas into the region of observations. Reference 82 shows the weakening and lowering, by 1/3, of the feathers height at the solar eclipse over India. Feathers are seen over the warm ocean on sodar record practically every time: in the region of Gulfstream in 80% (Ref. 2) or 84% (Ref. 29) of all observation time.

But the statistical analysis of long-term series of sodar data from the synoptic point of view has not been yet performed except for three papers. In Ref. 89 the frequency of occurrence of three types of images, referred to the Paskvill categories, was calculated separately for the conditions of anticyclone center or wedge. However, the separation of only one synoptic situation is little effective. Reference 24 demonstrates, using one month as an example, regular change of feathers height depending on the type of prevailing air mass and its temperature contrast with the underlying

surface. In Ref. 22, similar results for the height and frequency of occurrence of convective images were obtained already for five months of observation in different seasons in Moscow. However, the conclusions drawn there should be refined using a larger data sample.

9. SODAR OBSERVATIONS OF REGIONAL CLIMATIC PHENOMENA

Observations with the use of vertical sodars prove to be useful when studying certain types of atmospheric flows: chinuka in Canada,[70] harmattan in Nigeria,[36] summer monsoon in India,[82,83] summer and winter monsoons in Hong Kong,[62] sedimentation dynamics in subtropical anticyclone over the Mediterranean Sea,[68] etc. Sodars are also promising for studying local peculiarities in the ABL, for example, shore conditions influenced by breeze,[33] as well as some meteorological phenomena (dust storms in the Aral region,[13] etc.).

Sodar records are usually interpreted with 1-hour interval. This allows very accurate estimates of climatic characteristics of the ABL stratification to be obtained for such places, where continuous sounding was performed as long as during one year or longer. Such a statistics is accumulated for Tirupati[75] and New Delhi[81] (India; refined data can be found in Refs. 82 and 83), Krakov (Poland),[88] Beijing (China),[67] Moscow (USSR),[20–23,27] three sites in Greece,[39] and two sites in Great Britain.[85] The data for seven month of observations in Calgary (Canada) are published in Ref. 61. The primary interpretation of incomplete observations for one year in Tokyo (Japan) is presented in Ref. 52. Unfortunately, all these results are hard to compare because of the lack of a common technique for sodar data processing.

Other applications of acoustic sounding include monitoring of precipitation,[35] fog layer height,[45] gravitational waves passage in the near-ground inversion layer,[1] general wind shear in the ABL,[81] etc.

10. SODAR ESTIMATES OF THE MIXING LAYER HEIGHT

The mixing layer height is an important input parameter in model calculations of air pollution. But the classical Holtzvort method of MLH estimation from the data of T measurements with radiosondes and near ground has some strict limitations.[26, 37] The hopes for more accurate knowledge of this characteristic are connected with its prompt estimates with remote sounding methods, including sodar data. The reliability of such estimates and problems of agreement between them are considered in Refs. 48 and 84. Strictly speaking, sodar record shows the maximum possible value of pollutant distribution in vertical direction, rather than real distribution itself. In addition, the inversion top is not always impenetrable to overheated atmospheric pollutants.

Originally MLH was identified, on sodar record, with the bottom of inversion layer once it elevates off from the ground in the morning.[40,58] This situation, closed convection, is most clear and easy to interpret. Then MLH estimation from sodar data was expanded to other cases. MLH became to be identified with boundaries of any elevated[67] or near-ground[89] inversions. The MLH determination in daytime at convection, if there are no clearly closing layers on sodar records, is a more complicated problem. In this case in Refs. 5, 67, 75, and 89 the MLH is related to the feathers height, that gives strongly underestimated values; in Ref. 72 MLH is formally assumed to be equal to the sodar sounding range. In Ref. 46 the MLH is assumed to be equal to lowest of two heights: of the bottom of lowest cumulus cloud (or stratus cloudiness in the period of winter monsoon) and the inversion layer estimated from sodar data. If the sky is clear and layers cannot be seen on echograms, the usual calculation of MLH by Holtzvort is recommended. When assessing the technique from Ref. 46, we must give a credit to the logic of alternative approach. However, the bottom of Cu clouds in no way can be considered as a potential barrier for pollutants dispersal. The best sodar estimates of daytime MLH can be seemingly obtained by comparing the direct T measurements with the height of convective feathers on sodar records and introducing corresponding corrections to it.[11] The critical point for MLH estimations from sodar data (fortunately, quite rare one) is the neutral stratification, when there is no return signal on sodar records.

11. CONCLUSION

Summarizing the above-said, the conclusion can be drawn that vertical sodars, being compared with other devices for the ABL studies, have a lot of advantages. Among them are their economic feasibility, possibility of arranging continuous observations, highly detailed and resolved data of observations. However, it is desirable to support every time the analysis of temperature stratification from sodar facsimile images with simultaneous direct measurements in the ABL.

ACKNOWLEDGMENTS

The author would like to express his gratitude to M.A. Kallistratova for the proceedings of international symposia she placed at his disposal and M.A. Petrosyants for valuable advice.

This work was partially supported by the Russian Foundation for Fundamental Research (Project No. 95-051694).

REFERENCES

1. V.A. Andrianov, V.I. Vetrov, and B.V. Rakitin, in: *Proc. of the VI Int. Symp. on Laser and Acoustic Sounding*, Tomsk (1980), Part 2, pp. 142–146.

2. V.D. Belyavskaya et al., in: Preprint No. 7, Institute of Atmospheric Physics of the USSR Academy of Sciences, Moscow (1990), Part 1, pp. 55–61.
3. V.D. Belyavskaya et al., *ibid.*, Part 2, pp. 5–14.
4. N.L. Byzova, V.N. Ivanov, and E.K. Garger, *Turbulence in the Atmospheric Boundary Layer* (Gidrometeoizdat, Leningrad, 1989), 264 pp.
5. V.A. Gladkikh et al., Atmos. Oceanic Opt. **5**, No. 7, 473–477 (1992).
6. E.I. Grechko et al., Izv. Ros. Akad. Nauk, Fiz. Atmos. Okeana **29**, No. 1, 11–18 (1993).
7. A.E. Gur'yanov et al., Astronomich Zh. **65**, No. 3, 637–644 (1988).
8. V.P. Zhukov, V.N. Prilepov, and V.N. Puzaev, Tr. Tsentr. Gidrometeorol. Obs. **20(1)**, 124–132 (1984).
9. A.A. Isaev et al., Atmos. Oceanic Opt. **7**, No. 5, 342–349 (1994).
10. M.A. Kallistratova et al., Izv. Akad. Nauk SSSR, Fiz. Atmos. Okeana **20**, No. 2, 162–172 (1984).
11. M.A. Kallistratova et al., in: Preprint No. 1, Institute of Atmospheric Physics of the USSR Academy of Sciences, Moscow (1991), pp. 77–94.
12. M.A. Kallistratova, M.S. Pekour, and N.S. Time, in: Preprint No. 9, Institute of Atmospheric Physics of the Russian Academy of Sciences, Moscow (1992), Part 2, pp. 116–148.
13. D.V. Klimov et al., in: *Proc. of the II Session of the Russian Acoustic Society "Acoustic Monitoring of Media"*, Moscow (1993), pp. 210–212.
14. V.M. Kopeikin, V.N. Kapustin, and M.S. Pekour, Izv. Ros. Akad. Nauk, Fiz. Atmos. Okeana **29**, No. 2, 213–217 (1993).
15. V.I. Kornienko and V.V. Smirnov, Trudy Inst. Eksp. Meteorol. **51(142)**, 87–93 (1990).
16. N.P. Krasnenko, *Acoustic Sounding of the Atmosphere* (Nauka, Novosibirsk, 1986), 168 pp.
17. N.P. Krasnenko, V.A. Fedorov, and M.G. Fursov, in: *Proc. of the VI All-Union Symp. on Laser and Acoustic Sounding of the Atmosphere,* Tomsk (1980), Part 2, pp. 135–138.
18. N.P. Krasnenko and M.G. Fursov, in: Preprint No. 7, Institute of Atmospheric Physics AS USSR, Moscow, Part 1, pp. 30–33 (1990).
19. N.P. Krasnenko and M.G. Fursov, Atmos. Oceanic Opt. **5**, No. 6, 412–414 (1992).
20. M.A. Lokochshenko, Meteorol. Gidrol., No. 6, 54–65 (1994).
21. M.A. Lokochshenko, Meteorol. Gidrol., No. 7, 24–38 (1994).
22. M.A. Lokochshenko, Vestnik MGU, Geografiya, No. 4, 43–51 (1995).
23. M.A. Lokochshenko and M.S. Pekour, Atmos. Oceanic Opt. **5**, No. 3, 205–207 (1992).
24. M.A. Lokochshenko et al., Atmos. Oceanic Opt. **7**, No. 7, 522–527 (1994).
25. V.E. Ostashev, *Propagation of Sound in Moving Media* (Nauka, Moscow, 1992), 208 pp.
26. M.S. Pekour, in: Preprint No. 7, Institute of Atmospheric Physics AS USSR, Moscow (1990), Part 1, pp. 15–29.
27. M.S. Pekour, *ibid.*, pp. 62–71.
28. M.S. Pekour and M.A. Lokochshenko, in: *Proc. of the II Session of the Russian Acoustic Society "Acoustic Monitoring of Media"*, Moscow (1993), pp. 142–144.
29. I.V. Petenko, *ibid.*, pp. 66–67.
30. V.I. Tatarskii, *Wave Propagation in a Turbulent Medium* (McGraw Hill, New York, 1961).
31. N.S. Time et al., in: Preprint No. 7, Institute of Atmospheric Physics AS USSR, Moscow (1990), Part 2, pp. 15–19.
32. N.L. Byzova, ed., *Typical Characteristics of the Lower 300-meter Atmospheric Layer from Measurements from High Mast* (State Meteorological Institute Publishing House, Moscow, 1982), 68 pp.
33. Yu.N. Ul'yanov et al., in: Preprint No. 7, Institute of Atmospheric Physics AS USSR, Moscow (1990), Part 1, pp. 47–54.
34. M. Hayashi and A. Ikeda, Kogai **14**, Nos. 5–6, 263–277 (1981) [Russian translation].
35. L.G. Shamanaeva, in: *Proc. of the VI All-Union Symp. on Laser and Acoustic Sounding of the Atmosphere*, Tomsk (1980), Part 2, pp. 146–149.
36. J.A. Adedokun, in: *Proc. of the 6th Int. Symp. on Acoustic Remote Sensing,* Athens, Greece (1992), pp. 321–326.
37. R. Aron, Atm. Environ. **17**, No. 11, 2193–2197 (1983).
38. D.N. Asimakopoulos, in: *Proc. of the 5th Int. Symp. on Acoustic Remote Sensing of the Atmosphere and Oceans*, New Delhi (1990), pp. 75–87.
39. D.N. Asimakopoulos, C.G. Helmis, and D.G. Deligiorgi, Int. J. of Remote Sensing **15**, No. 2, 383–392 (1994).
40. R.A. Baxter, M.W. Chan, and J.C. Marlia, in: *Proc. of the Int. Symp. on Acoustic Remote Sensing of the Atmosphere and Oceans*, Calgary (1982).
41. D.W. Beran and F.F. Hall, Bulletin Am. Meteorol. Soc. **55**, No. 9, 1097–1105 (1974).
42. F. Beyrich, D. Kalass, and U. Weisensee, in: *Proc. of the 7th Inter. Symp. on Acoustic Remote Sensing*, USA (1994), pp. 6–11–6–16.
43. I.A. Bourne and T.D. Keenan, Nature **251**, Sept. 20, 206–208 (1974).
44. E.H. Brown and F.F. Hall, Reviews of Geoph. and Space Physics **16**, No. 1, 47–110 (1978).
45. S.J. Caughey, W.M. Dare, and B.A. Crease, Meteorological Magazine **107**, 103–112 (1978).
46. W.L. Chang and S. Lau, in: *Proc. of the 5th Int. Symp. on Acoustic Remote Sensing of the Atmosphere and Oceans,* New Delhi (1990), pp. 500–505.
47. G.H. Clark, E. Charash, and E.O.K. Bendun, J. Appl. Meteorol. **16**, 1365–1368 (1977).
48. R.L. Coulter, J. Appl. Meteorol. **18**, 1495–1499 (1979).

49. B. Crease, S. Caughey, and D. Tribble, Meteorological Magazine **106**, 42–52 (1977).
50. W.T. Cronenwett, G.B. Walker, and R.L. Inman, J. Appl. Meteorol. **11**, No. 12, 1351–1358 (1972).
51. F. Fanaki, in: *Proc. of the Int. Symp. on Acoustic Remote Sensing of the Atmosphere and Oceans*, Calgary (1982), pp. VII–19 – VII–34.
52. M. Fukushima, K. Akita, and H. Tanaka, J. Meteorol. Soc. Japan **52**, No. 5, 428–438 (1974).
53. B.S. Gera and A. Weill, in: *Proc. of the 4th Symp. of the Int. Soc. of Acoustic Remote Sensing*, Canberra, Australia (1988).
54. G.W. Gilman, H.B. Coxhead, and F.H. Willis, J. Acoust. Soc. Am. **18**, No. 2, 274–283 (1946).
55. R.G. von Gogh and P.Zib, J. Appl. Meteorol. **17**, No. 1, 34–39 (1978).
56. A.K. Goroch, J. Appl. Meteorol. **15**, No. 5, 520–521 (1976).
57. E. Gossard et al., J. Atm. Sci. **42**, No. 20, 2156–2169 (1985).
58. D. Guedalia et al., J. Appl. Meteorol. **19**, No. 7, 839–848 (1980).
59. F.F. Hall, J.C. Edinger, and W.D. Neff, J. Appl. Meteorol. **14**, No. 6, 513–523 (1975).
60. M. Hayashi, J. Meteorol. Soc. Japan **58**, No. 3, 194–201 (1980).
61. R.B. Hicks et al., Boundary-Layer Meteorol., No. 12, 201–212 (1977).
62. E. Hui Koo, W.L. Chang, and C.M. Tam, in: *Proc. of the 2nd Int. Symp. on Acoustic Remote Sensing of the Atmosphere and Oceans,* Rome (1983).
63. M.A. Kallistratova et al., Z. Meteorolog. **36**, No. 4, 229–237 (1986).
64. M.A. Kallistratova, in: *Proc. of the 6th Int. Symp. on Acoustic Remote Sensing of the Atmosphere and Oceans*, Athens (1992).
65. C.G. Little, Proc. IEEE **57**, No. 4, 571–578 (1969).
66. C.G. Little, in: *Proc. of the 4th Symp. of the Int. Soc. of Acoustic Remote Sensing,* Canberra (1988).
67. Lu Naiping et al., in: *Proc. of the 5th Int. Symp. on Acoustic Remote Sensing of the Atmosphere and Oceans,* New Delhi (1990), pp. 345–356.
68. A. Manes et al., in: *Proc. of the 4th Symp. of the Int. Soc. of Acoustic Remote Sensing,* Canberra (1988).
69. A. Marzorati, G. Mastrantonio, and G. Fiocco, *ibid.*
70. T. Mathews and P.F. Lester, in: *Proc. of the 2nd Int. Symp. on Acoustic Remote Sensing of the Atmosphere and Oceans*, Rome (1983).
71. R.A. Maughan, Atm. Environ., 13, 1697–1706 (1979).
72. R.A. Maughan, A.M. Spanton, and M.L. Williams, Atm. Environ. **16**, No. 5, 1209–1218 (1982).
73. L.G. McAllister, J. Atm. & Terrestrial Physics **30**, 1439–1440 (1968).
74. L.G. McAllister et al., Proc. IEEE **57**, No. 4, 579–587 (1969).
75. D. Narayana Rao et al., in: *Proc. of the 5th Int. Symp. on Acoustic Remote Sensing of the Atmosphere and Oceans,* New Delhi (1990), pp. 401–406.
76. W.D. Neff, Antarctic J. of the United States **13**, No. 4, 179–181 (1978).
78. M.S. Pekour and M.A. Kallistratova, Appl. Phys. **B56**, 1–7 (1993).
79. B.E. Prater and J.J. Colls, Atm. Environ. **15**, No. 5, 793–798 (1981).
80. P.B. Russel and E.E. Uthe, Atm. Environ. **12**, 1061–1074 (1978).
81. S.P. Singal, S.K. Aggarwal, and B.S. Gera, Mausam **33**, No. 4, 439–444 (1982).
82. S.P. Singal, B.S. Gera, and S.K. Aggarwal, J. of Scient. & Industr. Res. **43**, 469–488 (1984).
83. S.P. Singal et al., Atm. Environ. **19**, No. 2, 221–228 (1985).
84. S.P. Singal, J. of Scient. & Industr. Res. **47**, 520–533 (1988).
85. A.M. Spanton and M.L. Williams, Atm. Environ. **22**, No. 2, 211–223 (1988).
86. A.D. Surridge, New Zealand J. of Science **23**, No. 3, 283–288 (1980).
87. A.D. Surridge, in: *Proc. of the 5th Int. Symp. on Acoustic Remote Sensing of the Atmosphere and Oceans,* New Delhi (1990), pp. 482–489.
88. J. Walczevski and M. Felesky-Bielak, Atm. Environ. **22**, No. 9, 1793–1800 (1988).
89. J. Walczewski, in: *Proc. of the 5th Int. Symp. on Acoustic Remote Sensing of the Atmosphere and Oceans,* New Delhi (1990), pp. 477–481.
90. A. Weill, in: *Proc. of the Int. Symp. on Acoustic Remote Sensing of the Atmosphere and Oceans,* Calgary (1982).
91. R.J. Wyckoff, D.W. Beran, and F.F. Hall, J. Appl. Meteorol. **12**, No. 4, 1196–1204 (1973).